



1                   **Holocene and Common Era sea level changes in the Makassar Strait, Indonesia**  
2   Maren Bender<sup>1</sup>, Thomas Mann<sup>2</sup>, Paolo Stocchi<sup>3</sup>, Dominik Kneer<sup>4</sup>, Tilo Schöne<sup>5</sup> Jamaluddin Jompa<sup>6</sup>,  
3   Alessio Rovere<sup>1</sup>  
4   1 University Bremen, MARUM – Center for Marine Environmental Sciences, Leobener Straße 8, 28359  
5   Bremen, Germany  
6   2 ZMT – Leibniz Centre for Tropical Marine Research, Fahrenheitsstraße 6, 28359 Bremen, Germany  
7   3 NIOZ – Royal Netherlands Institute for Sea Research, 17907 SZ 't Horntje, Texel, Netherlands  
8   4 Alfred Wegener Institute, Helmholtz Centre for Polar and Marine Research, Hafenstrasse 43, 25992  
9   List / Sylt, Germany  
10  5 Helmholtz-Zentrum Potsdam – Deutsches GeoForschungsZentrum (GFZ), Telegrafenberg 14473  
11  Potsdam, Germany  
12  6 Graduate School, Hasanuddin University, Makassar, 90245, Indonesia

13

14   Keywords: GIA, microatolls, Spermonde Archipelago

15

16

17

18

19

20

21

22

23

24

25

26

27

28

29

30

31

32

33



34

35

36

37 Abstract

38 Indonesia is a country composed of several thousand islands, many of them small, low-lying and  
39 densely inhabited. These are, in particular, subject to high risk of inundation due to future relative sea  
40 level changes. The Spermonde Archipelago, off the coast of Southwest Sulawesi, consists of more than  
41 100 small islands. This study presents a dataset of 24 sea-level index points from fossil microatolls,  
42 surveyed on five islands in the Spermonde Archipelago and compares these new results with published  
43 data from the same region and with relative sea level predictions from different Glacial Isostatic  
44 Adjustment (GIA) models. The newly surveyed fossil microatolls are located around the islands of  
45 Tambakulu, Suranti (both ~60 km offshore of Makassar city), Bone Batang and Kodingareng Keke (both  
46 located in the center of the Archipelago) and Sanrobengi (located ~20 km south-southwest of  
47 Makassar). Results from the near- and mid-shelf islands indicate that relative sea level between 4 to 6  
48 ka BP was less than one meter above present sea level. The only exception to this pattern is the heavily  
49 populated island of Barrang Lompo, where we record a significant subsidence when compared to the  
50 other islands. These new results support the conclusions from a previous dataset and are relevant to  
51 constrain late Holocene ice melting scenarios. Samples from the two outer islands (Tambakulu and  
52 Suranti) yielded ages spanning the Common Era that represent, to our knowledge, the first reported  
53 for the entire Southeast Asian region.



54 1. Introduction

55 Sea-level rise is one of the main consequence associated with climate change, and is a major threat for  
56 coastal populations all over the globe (IPCC, 2014). In fact, more than half of the human population  
57 lives on low-lying islands or along coastlines (Houghton et al, 1996), and it has been estimated that, by  
58 2050, the frequency of coastal flooding may double (Vitousek et al., 2017). Due to the vulnerability of  
59 low-lying coastlines and islands to flooding or drowning (Nicholls et al., 1999; Nicholls and Cazenave,  
60 2010) it is essential to understand sea-level variability and its rates at different time scales (Lambeck  
61 and Chappell, 2001; Milne et al., 2009).

62

63 With the onset of the Holocene (~12 ka BP), after the Last Glacial Maximum, eustatic sea level rose as  
64 a result of increasing temperatures and ice loss in polar regions. Locally, sea level departs from the  
65 global average due to the combined effects of glacial isostatic adjustment (GIA) (Milne and Mitrovica,  
66 2008), including ocean syphoning (Milne and Mitrovica, 2008; Mitrovica and Milne, 2002; Mitrovica  
67 and Peltier, 1991) and the redistribution of water masses due to changes in gravitational attraction  
68 and Earth rotation following ice mass loss (Kopp et al., 2015). These processes are superimposed to  
69 land level changes due to geological processes, such as subsidence resulting from sediment  
70 compaction or tectonics (e.g., Tjia et al. (1972) and Zachariasen, (1998)). Sea-level reconstructions in  
71 areas far from polar regions (i.e., far-field, Khan et al., 2015) show a rapid sea-level rise after the onset  
72 of Holocene, followed by a GIA-driven sea level highstand in many equatorial areas between 6 and ~3  
73 ka BP (when ice melting was at its maximum), and a subsequent sea-level fall. Thus, far-field locations  
74 experienced a higher relative sea level (RSL) in the middle Holocene (e.g. Grossman et al., 1998; Mann  
75 et al., 2016) until ice melting rates decelerated.

76

77 In most tropical areas, Holocene RSL changes can be reconstructed using several types of RSL indicators  
78 (Khan et al., 2015), among which are fossil coral microatolls (e.g. (Scoffin and Stoddart, 1978;  
79 Woodroffe et al., 2012; Woodroffe et al. 2014). Microatolls live at Mean Lower Low Water (MLLW),  
80 but their living range can span from MLW and LAT. They grow upwards until their polyps reach MLLW,  
81 and keep growing horizontally at the same elevation, as soon as they reached this level. If sea level  
82 rises above MLW or falls below LAT over extended periods of time, the coral polyps die, retaining their  
83 fossil skeleton only. Due to this characteristic, fossil microatolls are often considered as an excellent  
84 RSL indicator, when found in good preservation state, as they constrain paleo RSL within MLW to LAT  
85 (Meltzner and Woodroffe, 2014). Fossil microatolls can also be easily assigned with an age, either by  
86 <sup>14</sup>C (Woodroffe et al., 2012) or U-series dating (Azmy et al., 2010). Recent studies also showed that the  
87 accurate measurement, dating and standardized interpretation of coral microatolls has the further  
88 potential to detail patterns and cyclicities related to short-term Holocene sea level fluctuations  
89 (Hallmann et al., 2018; Meltzner et al., 2017).

90

91 A recent review of sea level index points in SE Asia, the Maldives, India and Sri Lanka (Mann et al.,  
92 under rev.) show that, in these regions, microatolls represent ~27% of the 213 sea level index points  
93 reported by 31 studies. A study focusing on the Spermonde Archipelago (Mann et al., 2016) reported  
94 20 fossil and 1 modern microatoll on two islands located in the center of the Spermonde Archipelago,  
95 SW Sulawesi, Indonesia. In our study, we complement this existing dataset with 24 new fossil  
96 microatolls from five additional islands, located up to ~40 km South and ~42 km West from the islands  
97 studied by Mann et al. (2016), therefore providing RSL evidence across the entire Spermonde  
98 Archipelago.

99

100 This study aims to contribute to the current knowledge on late-Holocene relative sea level changes in  
101 the Spermonde Archipelago. We focus on newly sampled fossil microatolls (FMA) of five islands in the

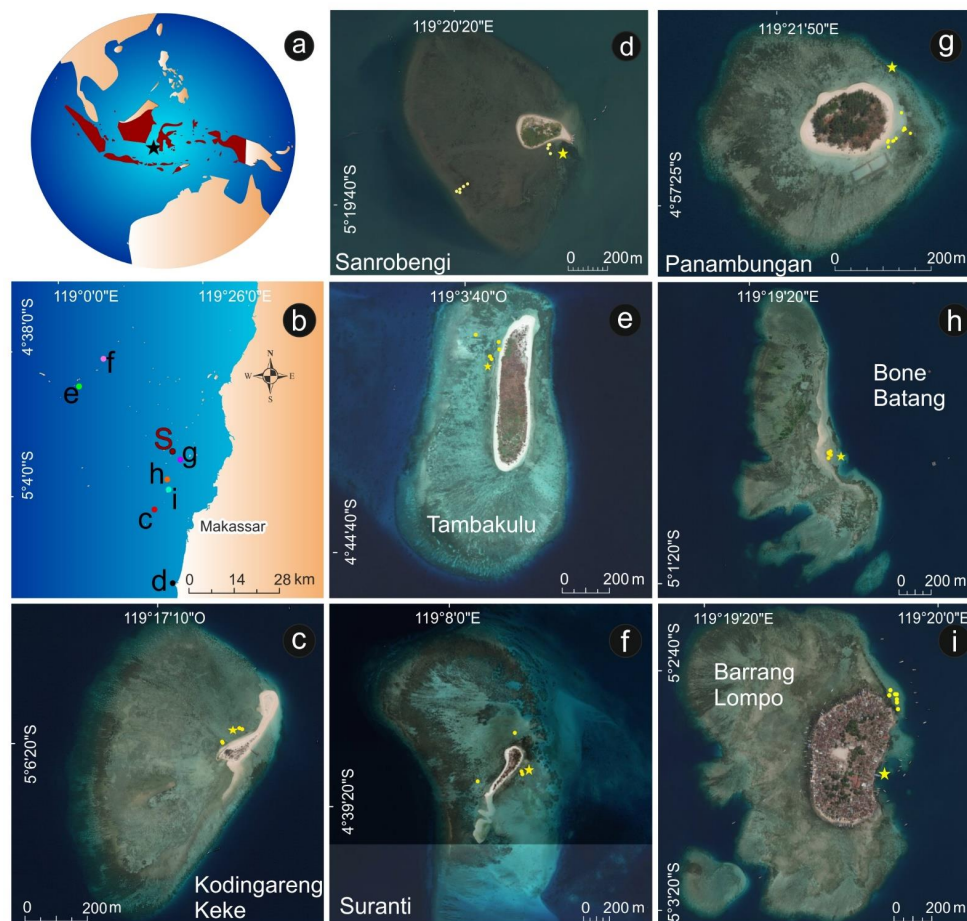


102 Archipelago, comparing them with two available datasets from Panambungan, an uninhabited island  
103 located 22 km to the northwest of Makassar (Figure 1g) and Barrang Lompo (Figure 1i) (Mann et al.,  
104 2016). The latter is densely populated and situated 14 km offshore from Makassar.  
105

## 106 2. Regional Setting

107 Indonesia consists mostly of small and low-lying Islands and coastlines, and includes roughly 15-17.000  
108 islands. The biggest island is Sumatra (~473.000 km<sup>2</sup>), while the smallest ones are less than 0.2 km<sup>2</sup> in  
109 size. The area of the Spermonde Archipelago, located between 4°00'S to 6°00'S and 119°00' E to  
110 119°30' E, hosts more than one hundred low-lying islands, with averaged elevations of 2 to 3 m above  
111 sea level (Janßen et al., 2017; Kench and Mann, 2017). All islands consist of fringing reefs bordering  
112 sand and rubble accumulations (Sawall et al., 2011) and some are densely populated (Schwerdtner  
113 Mánñez et al., 2012). Their low elevation above MSL and the fact that they are composed mostly of  
114 calcareous sediments makes them vulnerable to sea level rise, waves and deficits in sediment supply  
115 (Kench and Mann, 2017). These reefs bordering these islands are ideal environments for the  
116 preservation of microatolls (Mann et al., 2016), but in literature, only a small amount of sea level proxy  
117 data was reported to date in the Spermonde Archipelago. Overall, three studies (Tjia et al., 1972; De  
118 Klerk, 1982; Mann et al., 2016) report 42 data points, divided into 22 index points, 18 marine limiting  
119 (i.e. facies indicating marine conditions) and two terrestrial limiting points (i.e. facies indicating  
120 terrestrial conditions). It is worth noting that some of the indicators reported in the Makassar Strait  
121 were flagged to be treated with caution in a recent review by Mann et al. (under rev.), mostly as they  
122 would indicate mutually inconsistent sea level histories. As an example: Tjia et al. (1972) shows a 6-  
123 plus meters sea-level highstand between 4-6 ka BP that Mann et al. (2016) did not confirm based on  
124 microatolls of the same age.  
125

126 The newly surveyed islands, shown in Figure 1, are briefly described hereafter. **Bone Batang** (Figure  
127 1h) is located south of Panambungan and north of Barrang Lompo. This island is a narrow, uninhabited  
128 sandbank. South of Barrang Lompo, and 13 km southwest from the city of Makassar, we probed  
129 **Kodingareng Keke** (Figure 1c), another uninhabited island. 25 km south of Kodingareng Keke lies the  
130 island of **Sanrobengi** (Figure 1d), a small, sparsely inhabited (there are less than 15 houses) reef island  
131 located close to the mainland of southern Sulawesi at the coast of Galesong, 21 km south of Makassar  
132 city. Sanrobengi is located south of the previous islands, which are close to each other off the coast of  
133 Makassar, towards the center of the Archipelago. The fourth and fifth study islands are located  
134 northwest of Makassar, bordering the edge of the Spermonde Archipelago. These two outer islands  
135 are **Suranti** (Figure 1f) and **Tambakulu** (Figure 1e) and both are uninhabited and located 58 km  
136 (Suranti) and 56 km (Tambakulu) from the City of Makassar. Another island already reported and  
137 studied by Mann et al. (2016) (Sanane) is included in this study only for the analysis of living microatolls,  
138 as fossil microatolls were not found on this island. Its location is 2.7 km northwest of Panambungan,  
139 and it is densely populated.  
140



141  
142 *Figure 1. Overview map of the islands investigated by this study and the two islands studied by Mann et al., 2016. The star in*  
143 *a) indicates the location of the Spermonde Archipelago, off the coast of southwestern Sulawesi; b) indicates the position of*  
144 *each island. All letters in b) refer to the aerial views of each island in insets c) to i). The red dot labelled “S” indicates the*  
145 *position of Pulau Sanane, where only living microatolls were surveyed. On insets c) to i), the yellow dots indicate the location*  
146 *of sampled fossil microatolls, while the yellow asterisks indicate the position of the tide pressure sensor. Imagery sources for*  
147 *panels a) and b): Global Self-consistent Hierarchical High-resolution Shorelines from Wessel and Smith (2004) and for c) to i):*  
148 *Esri, DigitalGlobe, GeoEye, Earthstar Geographics, CNES/Airbus DS, USDA, USGS, AeroGRID, IGN, and the GIS User Community.*

### 149 3. Methods

150 Fossil and living microatoll heights on Sanrobengi, Kodiangareng Keke, Bone Batang, Suranti and  
151 Tambakulu (Figure 1) were surveyed with an automatic level. Their elevations were initially referenced  
152 to locally deployed water level sensors acting as temporary benchmarks (stars in Figure 1c-i). These  
153 sensors were fixed to either jetties or living corals close to the survey sites and logged the tide levels  
154 at 30-second intervals. Tidal level differences between the sensors on the study islands were  
155 referenced to the tidal height of the water level sensor on Panambungan, for which we have the  
156 longest tide record of 8 days and 18 h. The Panambungan tidal readings were compared to readings at  
157 the national tide gauge at Makassar harbor to establish the reference of our sample sites to MSL. As a  
158 result of annual sea level variability, the mean tidal level at Makassar was slightly above the MSL  
159 (+0.035 m), during our surveys. Our local tide gauge readings were corrected accordingly. Despite the  
160 Makassar tide gauge is operated since 2011 only (hence providing a relatively short time record), we



161 compared this time series with our tidal records to estimate MLLW at our study sites. Following this,  
162 the long-term consistency and trend of the MSL was tested using radar altimetry data since 1993  
163 (Schöne et al., 2010), where the 19-year MSL trend is around 5mm/a, hence slightly above the global  
164 trend.

165  
166 From our elevation measurements, we calculated paleo RSL applying the concept of indicative meaning  
167 (Shennan, 1986) to coral microatolls, using as modern analog living microatolls that were measured in  
168 the field. We calculated RSL using the following formula:

$$RSL = E - HLC + Er$$

169  
170  
171 where **E** is the surveyed elevation of the fossil microatoll; **HLC** is the average height of living coral and  
172 **Er** is the estimated portion that was eroded from the upper fossil microatoll surface. The latter value  
173 was included in our calculation only in presence of visibly eroded microatolls. The mean thickness of  
174 living microatolls in the Spermonde was quantified by Mann et al. (2016) to  $0.48 \pm 0.19$  m. Thus, to  
175 reconstruct the original fossil microatoll elevation below MSL, we added the missing centimeters to  
176 the actual thickness of eroded fossil microatolls to reconstruct the thickness of  $0.48 \pm 0.19$  m.  
177  
178



179  
180 *Figure 2. Examples of a) non-eroded and b) eroded fossil microatoll at Sanrobengi.*

181 To quantify the error in the RSL calculation, we use the square root of the sum of squares of each single  
182 uncertainty term, following the formula:

$$\sigma_{RSL} = \sqrt{\sigma_{Bm}^2 + \sigma_E^2 + \sigma_{HLC}^2 + \sigma_{Er}^2}$$

183  
184  
185 where  $\sigma_{Bm}$  is the individual benchmark error that stems from referencing the local tide and pressure  
186 sensor elevation on each island to the tide and pressure sensor elevation of Panambungan. We  
187 calculated the elevation difference between the sensor of one island e.g., Sanrobengi and  
188 Panambungan (sensor elevation below MSL) to get the sensor elevation below MSL for Sanrobengi and  
189 repeated it for each island. Thus, this error is included five times (one per island);  $\sigma_E$  is the elevation  
190 error of the survey. Note that, if the automatic level had to be moved due to excessive distance from  
191 the benchmark to the measured point, this error is doubled. This had to be done for FMA 1 to 3 in  
192 Suranti (tripod was moved twice thus four times this error) and FMA 22 to 26 in Sanrobengi. The  $\sigma_{HLC}$   
193 is the standard deviation of the height of living coral and  $\sigma_{Er}$  is the uncertainty in the coral erosion, if  
194 the microatoll was eroded.  
195  
196

197 In order to calculate RSL at each island using a suitable modern analog, we measured HLC at each island  
198 or, in case there were no living microatolls found, at the closest neighboring island with living  
199 microatolls. We surveyed living microatolls on Tambakulu (n=51) and Sanrobengi (n=24). On Suranti,



200 Kodingareng Keke and Bone Batang, living microatolls were restricted in number and with partly  
201 reworked appearance, or completely absent. Therefore, to calculate RSL at this islands, we used HLC  
202 elevations from Tambakulu (n=51) for Suranti, from Panambungan (from Mann et al. (2016); n = 20)  
203 for Bone Batang, and from Barrang Lompo (from Mann et al. (2016); n=23) for Kodingareng Keke.

204  
205 Fossil microatolls were sampled by hammer and chisel or with a hand drill. Sub-samples from all  
206 samples were analyzed via XRD at the Central Laboratory for Crystallography and Applied Material  
207 Sciences (ZEKAM), University of Bremen, Germany, in order to detect possible diagenetic alterations  
208 of the aragonite coral skeleton. AMS radiocarbon dating and age calibration to calendar years before  
209 present (cal a BP) was done at Beta Analytic Laboratory, Miami, USA. We used the Marine 13  
210 calibration curve (Reimer et al., 2013) and a delta R value of  $0 \pm 0$  as recommended for Indonesia in  
211 Southon et al. (2002). In order to compare the new ages to the results from Mann et al. (2016), we  
212 recalculated their ages with the same delta R value. We used a different delta R value than Mann et  
213 al. (2016) as the value they adopted was measured in a marine reservoir in southern Borneo (Southon  
214 et al., 2002) more than 900 km away from our study site (delta R value of  $89 \pm 70$ ). There is no delta R  
215 value available between Sulawesi and southern Borneo that can be used for a radiocarbon age  
216 reservoir correction. Due to the long distance between Borneo and our study area and the presence  
217 of the Indonesian Throughflow between these two regions (Fieux et al., 1996) there are no bases to  
218 assume a similar delta R value between southern Borneo and the Spermonde Archipelago. Therefore  
219 we used the delta R value recommended in Southon et al. (2002) that was reported to be derived from  
220 unpublished data for the Makassar Strait Indonesia.

221  
222 We compare the RSL calculated from field data to RSL predicted by geophysical models of Glacial  
223 Isostatic Adjustment (GIA), that are based on the solution of the Sea Level Equation (Clark and Farrell,  
224 1976; Spada and Stocchi, 2007). We calculate GIA predictions using a suite of combinations of ice-  
225 sheets and solid Earth models (Table 1). The latter are self-gravitating, rotating, radially stratified,  
226 deformable and characterized by a Maxwell viscoelastic rheology. We discretize the Earth's mantle in  
227 three layers: Upper Mantle, Transition Zone (TZ) and Lower Mantle (LM). Each mantle viscosity profile  
228 is combined with a perfectly elastic lithosphere whose thickness ranges from 90 to 120 km (Figure 6).  
229 We combine the Earth models with ICE-5G ice-sheet model (Peltier, 2009) and ANICE ice-sheet model  
230 (De Boer et al., 2015, 2017) and compute the RSL curves at the sites.

231

232 *Table 1. Glacial Isostatic Adjustment models used in this study. UM - Upper Mantle (Pas), TZ - Transition Zone (Pas), LM -*  
233 *Lower Mantle (Pas), LT - Lithosphere thickness (km).*

Model name	UM	TZ	LM	LT
ICE5G-VM2-90	0.25	0.5	5	90
ICE5G-VM2B-90	0.25	0.25	5	90
ICE5G-VM2-120	0.25	0.5	5	120
ICE5G-VM3-90	0.25	0.5	10	90
ICE5G-VM4-90	0.25	0.5	100	90
ANICE-VM1-100	0.5	0.5	2	100
ANICE-VM2-100	0.5	0.5	5	100
ANICE-VM3-100	0.5	0.5	10	100

234

#### 235 4. Results

236 Our new dataset consists of 17 fossil microatolls with average ages in calendar years ranging from  
237  $5956.5 \pm 83.5$  a BP to  $3614.5 \pm 98.5$  a BP and 8 fossil microatolls with ages varying from  $236.5 \pm 96.5$  a BP  
238 to  $36.5 \pm 11.5$  a BP surveyed on five islands (Table 2). These are added to the 20 fossil microatolls and



239 one modern microatoll from Barrang Lompo and Panambungan previously reported by Mann et al.  
 240 (2016) (Table 3). During the survey, in comparison to other microatolls on Suranti the microatoll  
 241 PS\_FMA 4 showed evidences of reworking, e.g., its position is plainly deeper than the other fossil  
 242 microatoll positions on Suranti and it was not securely grounded, thus it was subsequently rejected.  
 243 Therefore, it is not shown in the results or discussed further.

244 As shown in Table 2 and Figure 3b, the fossil microatoll of Sanrobengi range in age from 5956.5±83.5  
 245 a BP to 3614.5±98.5 a BP, with RSL from 0.14±0.21 m to 0.54±0.28 m. At the same island, the average  
 246 HLC of 24 living microatolls is -0.36 m with a minimum elevation of -0.48±0.06 m and a maximum  
 247 of -0.17±0.06 m (Figure 4). Ages of microatolls sampled on the outer islands Tambakulu and Suranti  
 248 are different from the other islands. On Tambakulu, ages range between 36.5±11.5 a BP and 114±114  
 249 a BP. In this time span, the elevations of the fossil microatolls at this island indicate RSL positions  
 250 between -0.24±0.22 m and 0.11±0.29 m. The living microatoll survey on Tambakulu included 51  
 251 individuals showing a maximum elevation of -1.03±0.08 m and a minimum of -0.61±0.08 m. Samples  
 252 from Suranti show age ranges from 114±114 a BP to 236.5±96.5 a BP. These samples indicate paleo  
 253 RSL positions of -0.54±0.30 m and -0.12±0.29 m. Fossil microatoll ages from Kodongareng Keke vary  
 254 from 5868.5±98.5a BP to 5342.5±87.5 a BP, indicating paleo RSL positions between -0.04±0.21 m and  
 255 0.08±0.21 m. The samples from Bone Batang cover ages from 5196±118 to 3692.5±107.5 a BP and  
 256 provide paleo RSL positions of 0.10±0.29 m to 0.17±0.29 m.

257 *Table 2. Fossil microatoll sampled at Sanrobengi (SB\_FMA 18 – 26), Tambakulu (PT\_FMA 5 – 9), Suranti (PS\_FMA 1 – 3),*  
 258 *Kodingareng Keke (KK\_FMA 14 – 17) and Bone Batang (BB\_FMA 11 – 13). All ages are recalculated with the delta R value of*  
 259 *0 ± 0 (Southon et al., 2002).*

ID	Island	Mean Age (cal a BP)	Age error	MSL [m]	HLC [m]	RSL [m]	RSL uncertainty [m]
SB_FMA18	Sanrobengi	4954.5	109.5	-0.19	-0.36	0.14	0.21
SB_FMA19	Sanrobengi	5956.5	83.5	-0.11	-0.36	0.22	0.21
SB_FMA20	Sanrobengi	5509.5	66.5	-0.16	-0.36	0.50	0.28
SB_FMA21	Sanrobengi	5970	89	-0.12	-0.36	0.54	0.28
SB_FMA22	Sanrobengi	5550.5	77.5	-0.01	-0.36	0.32	0.22
SB_FMA23	Sanrobengi	4740.5	94.5	-0.01	-0.36	0.32	0.22
SB_FMA24	Sanrobengi	4488.5	91.5	0.00	-0.36	0.48	0.29
SB_FMA25	Sanrobengi	4453.5	92.5	-0.02	-0.36	0.46	0.29
SB_FMA26	Sanrobengi	3614.5	98.5	-0.02	-0.36	0.46	0.29
PT_FMA5	Tambakulu	95	95	-0.89	-0.77	-0.16	0.22
PT_FMA6	Tambakulu	114	114	-0.89	-0.77	-0.16	0.22
PT_FMA7	Tambakulu	112.5	112.5	-0.97	-0.77	-0.24	0.22
PT_FMA8	Tambakulu	36.5	11.5	-0.82	-0.77	0.11	0.29
PT_FMA9	Tambakulu	58	58	-0.95	-0.77	-0.09	0.29
PS_FMA1	Suranti	114	114	-1.47	-0.77	-0.54	0.30
PS_FMA2	Suranti	187.5	91.5	-1.21	-0.77	-0.15	0.29
PS_FMA3	Suranti	236.5	96.5	-1.18	-0.77	-0.12	0.29
KK_FMA14	Kodingareng Keke	5342.5	87.5	-0.46	-0.47	-0.03	0.21
KK_FMA15	Kodingareng Keke	5868.5	98.5	-0.47	-0.47	-0.04	0.21
KK_FMA16	Kodingareng Keke	5519.5	65.5	-0.35	-0.47	0.08	0.21
KK_FMA17	Kodingareng Keke	5519.5	65.5	-0.43	-0.47	0.00	0.21
BB_FMA11	Bone Batang	4869	75	-0.58	-0.50	0.17	0.29
BB_FMA12	Bone Batang	5196	118	-0.65	-0.50	0.12	0.29
BB_FMA13	Bone Batang	3692.5	107.5	-0.67	-0.50	0.10	0.29



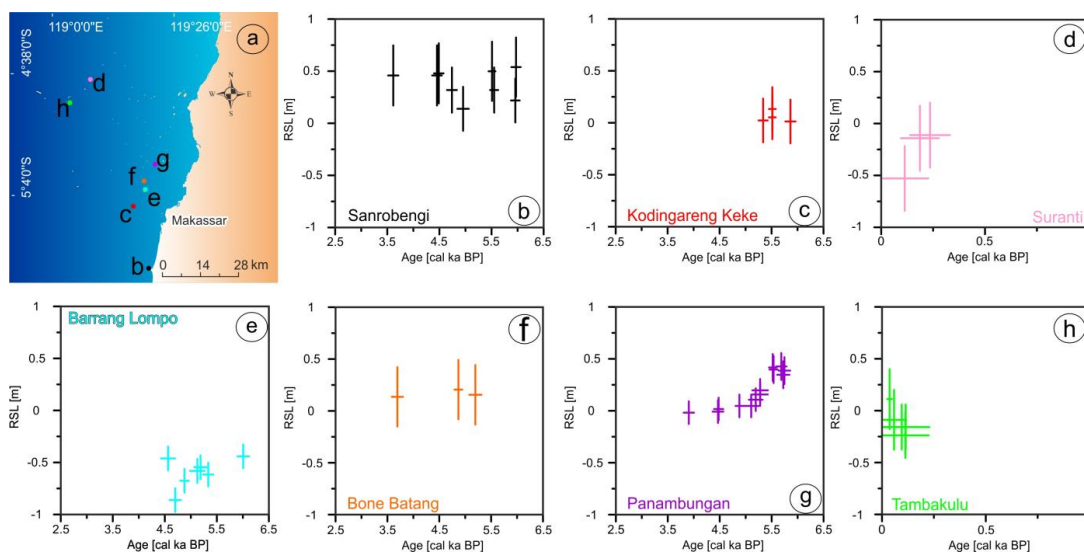
261 The recalculated fossil microatoll ages of Barrang Lompo (FMA 1 (BL) to FMA 7 (BL)) range from  
 262 4562±136 a BP to 6006.5±112.5 a BP and predict RSL positions between -0.86±0.09 m and -0.44±0.09  
 263 m. The modern counterparts (n= 23) show elevations between -0.59±0.05 m and -0.38±0.05 m below  
 264 MSL, which result in an average HLC of -0.47±0.05 m below MSL (Figure 4). Recalculated ages on  
 265 Panambungan (FMA 8 (PPB) – FMA 20 (PPB)) vary between 5746.5±109.5 a BP and 3905±100 a BP.  
 266 FMA 21 (PPB) is modern. RSL predictions for Panambungan range from -0.02±0.11 m to 0.23± 0.11 m.  
 267 On this study site, a survey of 20 living microatoll provides a minimum elevation of -0.70±0.07 m and  
 268 a maximum elevation of -0.42±0.07 m below MSL. The average HLC is -0.50±0.07 m below MSL (Figure  
 269 4).

270 *Table 3: This table reports the 21 fossil microatolls sampled by Mann et al. (2016) surveyed on Barrang Lompo (FMA 1 (BL) –*  
 271 *FMA 7 (BL)) and Panambungan (FMA 8 (PPB) – FMA 21 (PPB)). All ages are recalculated with a delta R value of 0 and an error*  
 272 *of 0 (Southon et al., 2002).*

ID	Island	Mean Age (cal a BP)	Age error	MSL [m]	HLC [m]	RSL [m]	RSL uncertainty [m]
FMA 1 (BL)	Barrang Lompo	4701	108	-1.35	-0.47	-0.86	0.11
FMA 2 (BL)	Barrang Lompo	6006.5	112.5	-0.93	-0.47	-0.44	0.11
FMA 3 (BL)	Barrang Lompo	4562	136	-0.95	-0.47	-0.46	0.11
FMA 4 (BL)	Barrang Lompo	5187	121	-1.03	-0.47	-0.55	0.11
FMA 5 (BL)	Barrang Lompo	5335	99	-1.10	-0.47	-0.62	0.11
FMA 6 (BL)	Barrang Lompo	4878	83	-1.16	-0.47	-0.68	0.11
FMA 7 (BL)	Barrang Lompo	5125	142	-1.07	-0.47	-0.58	0.11
FMA 8 (PPB)	Panambungan	5746.5	109.5	-0.30	-0.50	0.19	0.13
FMA 9 (PPB)	Panambungan	5537.5	78.5	-0.29	-0.50	0.20	0.13
FMA 10 (PPB)	Panambungan	5521	72	-0.27	-0.50	0.22	0.13
FMA 11 (PPB)	Panambungan	5686	101	-0.26	-0.50	0.23	0.13
FMA 12 (PPB)	Panambungan	5193	131	-0.38	-0.50	0.11	0.11
FMA 13 (PPB)	Panambungan	5278	150	-0.29	-0.50	0.20	0.11
FMA 14 (PPB)	Panambungan	3905	100	-0.50	-0.50	-0.02	0.11
FMA 15 (PPB)	Panambungan	4879	75	-0.44	-0.50	0.05	0.11
FMA 16 (PPB)	Panambungan	4479	88	-0.47	-0.50	0.02	0.11
FMA 17 (PPB)	Panambungan	4466.5	103.5	-0.49	-0.50	-0.01	0.11
FMA 18 (PPB)	Panambungan	5106.5	149.5	-0.44	-0.50	0.05	0.11
FMA 19 (PPB)	Panambungan	5279	146	-0.33	-0.50	0.16	0.11
FMA 20 (PPB)	Panambungan	5724	118	-0.34	-0.50	0.15	0.13
FMA 21 (PPB)	Panambungan	modern	modern	-0.44	-0.50	0.04	0.11

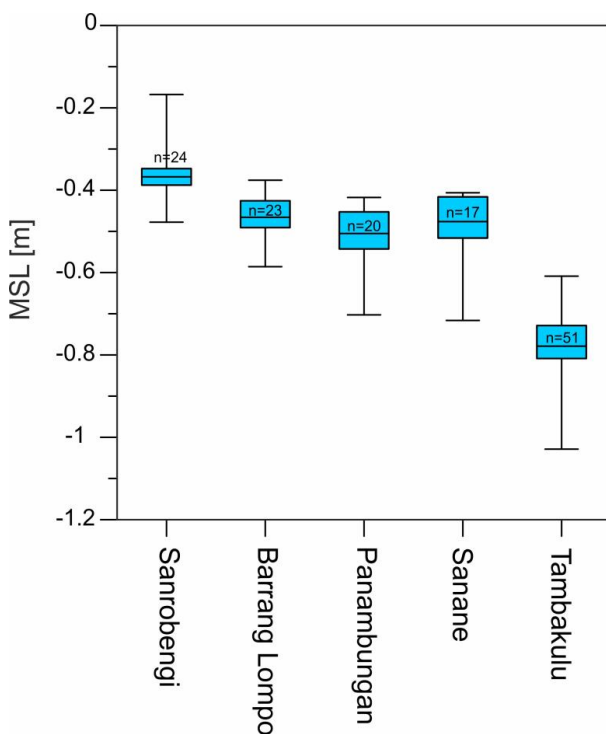
273

274 Data from Table 1 and Table 2 are plotted in Figure 3. The location of each study site is indicated in  
 275 Figure 3a) by letters and dots that are representing the colors of the related graphs. Locally measured  
 276 HLC, used to calculate RSL as reported in the methods, is plotted in Figure 4.



277

278 *Figure 3. Holocene RSL data in the Makassar Strait. a) The locations of the islands where FMA were surveyed; panels b) to h)*  
 279 *RSL vs age of the sea-level indicators at each island. Note that, for a better visualization and because of the young age, the*  
 280 *x-axis for panel d) Suranti and h) Tambakulu is shorter than for the other islands, but the y-axis is unchanged.*



281

282 *Figure 4. Box plot of the HLC elevations measured in the Spermonde Archipelago; “n”= indicates how many individuals were*  
 283 *surveyed on each island.*



284 5. Discussion

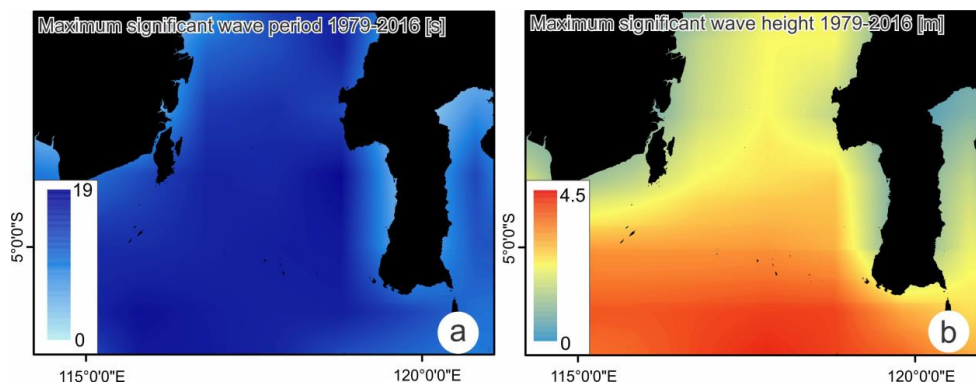
285 The dataset presented in Table 1 and Table 2 allows discussing five relevant points that need to be  
286 considered as Holocene sea level studies in the Makassar Strait and SE Asia progress.

287 5.1. Abandoning conflicting sea level histories

288 Additionally to our new dataset and that of Mann et al. (2016), there are two other studies reporting  
289 sea-level data for the Makassar Strait: De Klerk (1982) and Tjia et al. (1972). Both studies show a sea-  
290 level highstand in excess of 6 meters in the Makassar Strait, and only two points from De Klerk (1982)  
291 seem to be comparable with our dataset. The amassed quantity of new data agrees broadly with the  
292 observations from Mann et al. (2016) and provides further evidence that the mid-Holocene sea level  
293 highstand in the Makassar Strait was less than one meter above present sea level (Figure 6), *de facto*  
294 contradicting the studies cited above.

295 This raises an important question: why are the data from Tjia et al. (1972) and De Klerk (1982)  
296 significantly different from our reconstruction? A recent study by Mann et al. (under rev.) reviewed  
297 the original descriptions and interpreted these data as marine limiting points (i.e., indicating that sea  
298 level was above the measured point). This was based on the fact that the points reported in these  
299 studies are described as corals, shell accumulations, erosional terraces, oysters or mollusk deposits.  
300 These indicators might not represent valid sea level index points, and some were interpreted as marine  
301 limiting data, meaning that sea level was above the measured elevation of the geological facies  
302 reported. As a result, Mann et al. (under rev.) advise caution in using the data from older compilations  
303 in the Makassar Strait. Our dataset highlights that new studies are indeed necessary to unravel the  
304 process responsible for deposits at such high elevations as the data reported by Tjia et al. (1972) and  
305 De Klerk (1982).

306 One possibility, that would need further fieldwork and new stratigraphic analyses to be tested, is that  
307 these high marine deposits were emplaced by either storm or tsunami waves during the Holocene sea  
308 level highstand. For which concerns storm waves, the CAWCR wave hindcast (Durrant et al., 2013,  
309 2015) shows that the maximum significant wave heights in the proximity of the Spermonde  
310 Archipelago reached peaks of ~4 m, with periods of ~19 s in the period 1979-2016 (Figure 5).



311

312 Figure 5. Maximum significant wave period (a) and height (b) extracted from the CAWCR wave hindcast (Durrant et al., 2013,  
313 2015). CAWCR is an ocean wave hindcast that uses the WaveWatch III v4.08 wave model forced with NCEP CFSR hourly winds.  
314 Source: Bureau of Meteorology and CSIRO Copyright 2013.

315 Historical tsunami deposits are not unusual along the coasts of SE Asia (e.g. Rhodes et al., 2011) with  
316 the broader Makassar Strait being one of the most tsunamigenic regions in Indonesia (Harris and  
317 Major, 2017; Prasetya et al., 2001). For the center of the Makassar Strait, earthquake catalogs report  
318 only few significant earthquakes in the last ~100 years (Jones et al., 2014) and this region is considered



319 “the weakest amongst all of the seismic prone areas in Sulawesi” (Baeda, 2011). Nevertheless, three  
320 shallow earthquakes (depth below 20 km) in 1967, 1969 and 1984 generated tsunamis in this region  
321 (Prasetya et al., 2001). An earthquake on April 11<sup>th</sup> 1967 hit the town of Tinambung (140 km north of  
322 the Spermonde Archipelago) causing 58 deaths and 100 injured (Thein et al., 2014). During this  
323 tsunami, water retreat was reported but no tsunami wave height estimates are available. Another  
324 earthquake with the epicenter 215 km from the Spermonde Archipelago was reported on Feb 23<sup>rd</sup>  
325 1969, with wave heights of 2-6 m (Prasetya et al., 2001). It is unclear whether these events may have  
326 produced significant events also in the Spermonde Archipelago: the paleo record, together with  
327 tsunami wave models for these events, may help improving the current understanding of potential  
328 tsunami risks for this area, bringing paleo constraints to it (Kench and Mann, 2017).

#### 329 5.2. Validation of GIA models

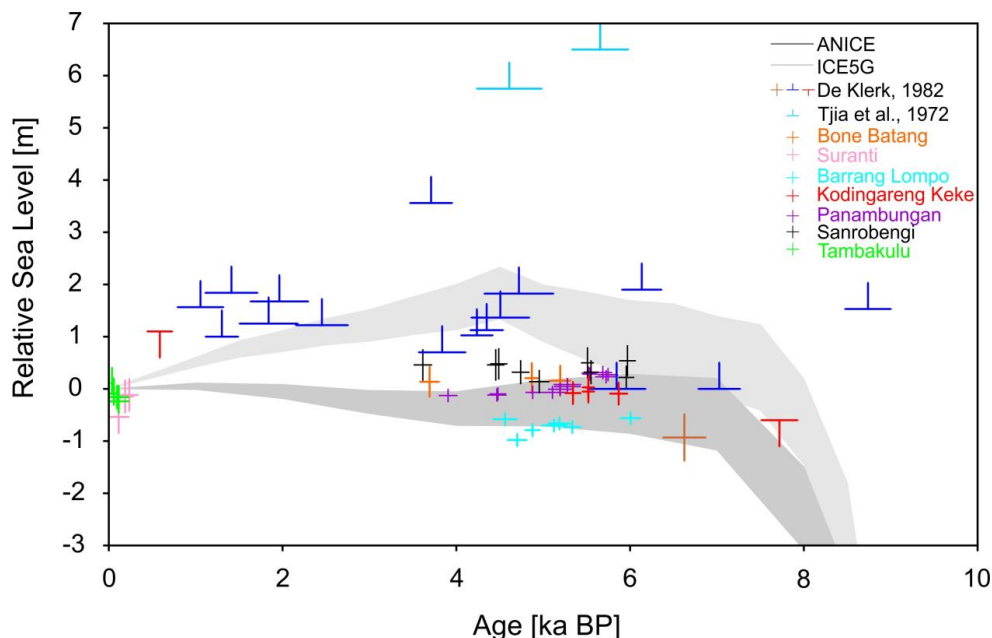
330 Under the assumption that tectonic activity did not play a major role in the Makassar Strait (Bird, 2003;  
331 Walpersdorf et al., 1998), the bulk of data presented in this paper (except those from Barrang Lompo,  
332 discussed below) may be used to validate the outputs of GIA models. This is in turn relevant to GIA  
333 corrections applied to tide gauge and satellite measurements aimed at quantifying the modern  
334 climate-related sea-level changes.

335 Comparing our data with GIA predictions based on ICE-5G (Peltier, 2004) (summarized as light gray  
336 band) (Figure 6), it is obvious that the model predicts a highstand that is up to 2 m higher than the bulk  
337 of our field data, and its peak is predicted to occur roughly 1.5 ka later than what our data suggest.  
338 The ANICE model performs better in this area, also considering that it was not generated by including  
339 RSL observations to calibrate the ice model. In general, it underestimates systematically the highstand  
340 by, at worst, half meter. Overall, the best performing model across all areas is ANICE-VM3-100, which  
341 predicts a maximum highstand of 0.28 m. Standing this result, we propose that future studies should  
342 explore different ice models (associated with a larger set of mantle viscosities) to gauge better fits and  
343 misfits to our sea level index points.

344 The better match of ANICE to our data has a meaning for which concerns ice melting patterns. In fact,  
345 the lower highstand predicted by ANICE stems from a very different (from the nominal ICE-5G model)  
346 behavior of the Antarctic Ice Sheet (AIS) component. In ANICE, the AIS undergoes a fluctuation  
347 throughout the Holocene, which might locally interfere with the syphoning effect, hence mitigating  
348 the Holocene highstand (followed by a quasi-linear drop) predicted by ICE-5G.



349



350

351 *Figure 6. RSL index points, marine and terrestrial limiting data available for the Makassar Strait, including GIA model*  
352 *outputs. The light gray band represents GIA predictions obtained using the five iterations of ICE-5G shown in Table 1 (Peltier,*  
353 *2004). The dark gray band represents GIA predictions obtained using the three iterations of ANICE shown in Table 1. The*  
354 *blue and light blue indicators from De Klerk (1982) and Tjia et al. (1972) indicate marine limiting indicators and the red*  
355 *symbol of the De Klerk, 1982 indicates a terrestrial limiting indicator. Crosses indicate sea level index points.*

### 356 5.3. Measuring living microatolls

357 As indicated in former studies (e.g. Mann et al., 2016; Smithers and Woodroffe, 2001; Woodroffe et  
358 al., 2012) it is important to measure the height of living corals (HLC) to determine the indicative  
359 meaning of fossil microatolls. Our results demonstrate the importance of HLC being measured in a  
360 similar context to the paleo HLC. Across the Spermonde Archipelago, we observed indeed a clear  
361 geographic trend in the measured HLC (Figure 4). The highest HLC (closer to mean sea level) was  
362 measured at the southernmost island (Sanrobengi), which is also the closest to the mainland. The  
363 islands located in the middle of the archipelago (Panambungan, Sanane and Barrang Lompo) differ  
364 slightly from each other but show comparable average HLC. At Tambakulu, located further away from  
365 the mainland (~70 km from Sanrobengi), the HLC is the lowest measured.

366 We propose that this difference is based on a mean sea level (and possible tidal range affecting the  
367 MLLW level) difference from the coast (Makassar tide gauge) to open ocean, due to a progressively  
368 deepening general bathymetry, and there is no reason to assume that this gradient was different  
369 during the Late Holocene. Had we not taken into account this effect, our RSL estimates would have  
370 been biased. This result reinforces the importance of defining local modern analogues to calculate  
371 paleo RSL from coral microatolls (Hallmann et al., 2018; Woodroffe, 2003). We highlight that the  
372 maximum difference we found between living microatolls at different sites in our study area (i.e., ~40  
373 cm, Figure 4) is of the same magnitude (several decimeters) with those measured at different sites  
374 by other studies (Hallmann et al., 2018; Smithers and Woodroffe, 2001; Woodroffe, 2003; Woodroffe et  
375 al., 2012). This indicates that, if no local living microatolls are measured contextually to fossil ones,  
376 there is the potential that paleo RSL reconstructions may be biased, in the worst case, by several  
377 decimeters.

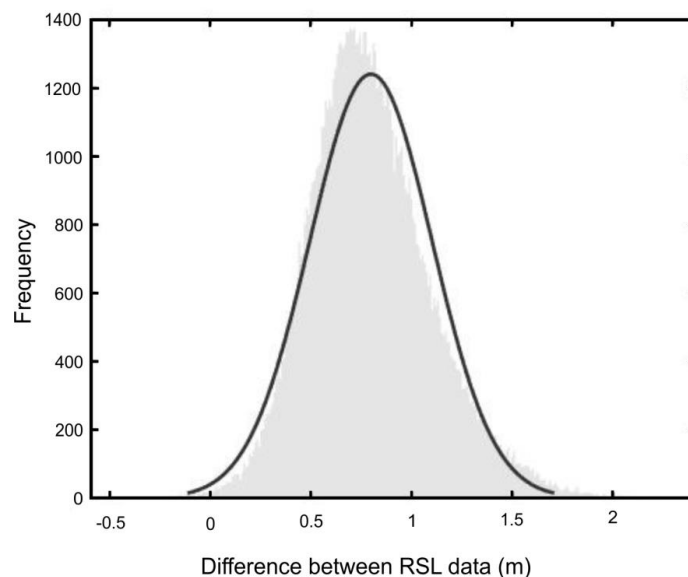


378 5.4. Local subsidence effects

379 As described above, the data presented in this study together with the data from Mann et al. (2016),  
380 confirm a sea level history with a sea level highstand 3.5-6 ka BP. The only exception to this pattern is  
381 the island of Barrang Lompo where microatolls of roughly the same age are consistently lower (Figure  
382 6). Comparing the data at Barrang Lompo with those from the other islands, we calculate that, on  
383 average, Barrang Lompo RSL data is  $0.8 \pm 0.3$  m lower than all the other islands where we surveyed  
384 microatolls of the same age (Figure 7).

385 While some GIA models (specifically those not predicting an highstand in our study area, ANICE-VM1-  
386 100 and ANICE-VM2-100, see supplementary materials for details) match the lower RSL recorded at  
387 Barrang Lompo, the better matching of other models (specifically ANICE-VM3-100) on multiple islands  
388 in close proximity with Barrang Lompo (Bone Batang - 3.7 km, Panambungan - 10.8 km and  
389 Kodingareng Keke - 7.7 km) stands as a good reason to infer that Barrang Lompo is indeed subject to  
390 subsidence.

391 The reason for this subsidence is presently unknown, but there is one striking geographic characteristic  
392 that separates Barrang Lompo from the other islands reported in this study. Among all the islands we  
393 surveyed, Barrang Lompo is the only heavily populated one (~4.5 thousand people) (Syamsir et al.,  
394 2019). It is characterized by a very dense network of buildings and concrete docks to allow fishing boats  
395 to land. All the fossil microatolls reported in Mann et al. (2016) were located near the coast, and might  
396 have been therefore affected by subsidence due to the combined effects of groundwater extraction  
397 (at least 8 wells were reported on Barrang Lompo, Syamsir et al., 2019) and loading of buildings on the  
398 coral island. The living microatolls, surveyed on the modern reef flat few hundred meters away from  
399 the island, do not show effects of subsidence.



400

401 *Figure 7. Difference in fossil microatoll elevations between the islands showing a Holocene sea level highstand above MSL*  
402 *and Barrang Lompo. For the methodology on how this figure was generated, the reader is referred to the matlab script*  
403 *contained in the following repository: <https://github.com/Alerovere/HoloceneVerticalMovements>*

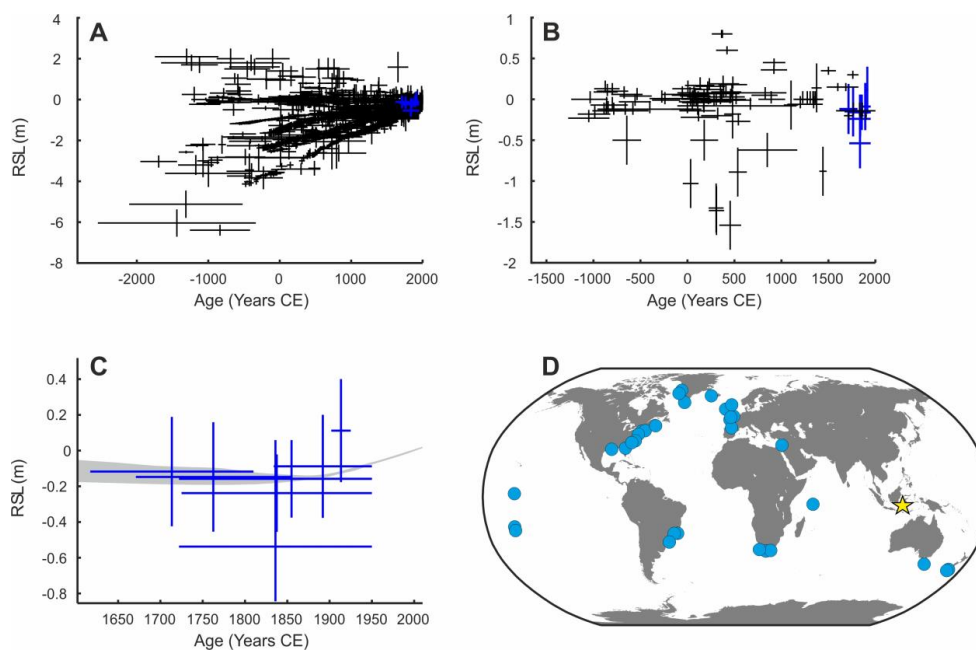
404 5.5. A Common Era sea level record from SE Asia?

405 One further interesting aspect of our study is that eight microatolls returned ages spanning the last  
406 four centuries. This period of time is included in the Common Era (that spans ca. the last 2 ka), that is



407 a particularly relevant time frame from the point of view of sea level changes as it marks the boundary  
408 between the tide gauge record and paleo proxies (Kopp et al., 2016). If compared with the entire  
409 Holocene, relatively few data have been published for the Common Era (1344 index points, see  
410 Supplementary Data in Kopp et al., 2016 also shown in Figure 8a). Most of these were surveyed in the  
411 US Atlantic coast and Gulf of Mexico (Figure 8d, 624 data points), while the only Common Era data in  
412 tropical areas were surveyed in the Indo-Pacific (Seychelles, Woodroffe et al., 2015) and in Pacific  
413 Ocean islands (Christmas Island, Kiribati and the Cook Islands, Goodwin and Harvey, 2008; Mcgregor  
414 et al., 2011; Woodroffe et al., 2012) (Figure 8b).

415 The eight data points presented in this study are, to our knowledge, the first report of Common Era  
416 data from Southeast Asia. Comparing the RSL obtained from our microatolls with the RSL by Kopp et  
417 al. (2016), we show that the elevations of six microatolls (PS\_FMA2 and 3 and PT\_FMA5, 6, 7 and 9)  
418 are consistent with his model, while other two (PT\_FMA8 and PS\_FMA1) are either too low or too high  
419 (Figure 8c). The six microatolls fitting in the modeled RSL range in elevation from  $-0.24 \pm 0.22$   
420 to  $-0.09 \pm 0.29$  m. Although this comparison does not take into account the fact that our paleo RSL  
421 should be corrected for GIA, we also maintain that this is a potentially little effect over such short time  
422 scales.



423

424 *Figure 8. A) Age-elevation plot of all Common Era data as compiled by Kopp et al. (2016) (1344 data points). The blue*  
425 *markers indicate the Common Era microatolls dated in this survey; B) Same as in A), but limited to the data available for the*  
426 *Indo-Pacific and Pacific Ocean Islands; C) the eight data points reported in this study (blue markers) compared with the*  
427 *ML21 and ML22 models of sea level from Kopp et al. (2016); D) Location of the Common Era data compiled by Kopp et al.*  
428 *(2016). The star indicates the location of the study area addressed by this paper.*

## 429 6. Conclusion

430 Our study allows us to draw few main conclusions for which concerns sea level changes in the Makassar  
431 Strait.

- 432 1. The data amassed collectively by this study and Mann et al. (2016) shows the Middle Holocene  
433 sea level highstand in the Spermonde Archipelago is less than one meter above modern sea



434 level. It is still necessary to find different explanations for the ~4m higher marine deposits  
435 identified by former studies in this area (De Klerk, 1982; Tjia et al., 1972). Such explanation  
436 may open new research directions in terms of paleo storms or tsunamis in this region. For  
437 which concerns GIA, the ICE-5G model modulated with differing mantle viscosities show a  
438 mismatch with our RSL results. The predicted RSL is higher than the RSL derived from our  
439 samples, and appears also shifted in time. Some iterations of ANICE seem to perform better.  
440 The differences between ICE-5G and ANICE are mainly due to a different modeling of Antarctic  
441 Ice Sheet evolution post 6 ka hence we argue that more ice and earth models should be made  
442 available to compare with our RSL data in search for a better match.

443 2. There is an obvious geographic trend in the Height of Living Corals (HLC) we measured on living  
444 microatolls. These HLC differences are probably based on differences in mean sea level and  
445 tidal regimes due to a changing bathymetry from the coast towards the open ocean that need  
446 to be tested via independent data (e.g. longer local tide gauge data).

447 3. The enigmatic low elevation of Late Holocene microatolls on the inhabited island of Barrang  
448 Lompo, already raised by Mann et al. (2016), is confirmed as an exception to a well-established  
449 pattern from other four sparsely located islands. We propose that the low elevation of these  
450 microatolls may be due to local subsidence caused by intensive human occupation of the  
451 island, with subsequent groundwater extraction. This subsidence has the potential to  
452 exacerbate, in the future, the effect of ongoing sea-level rise

453  
454 4. Eight of our 24 fossil microatolls date to the Common Era. Sea-level index points of that age  
455 were found in several locations but ours are, to the best of our knowledge, the first reported  
456 for Southeast Asia. At present state, we recognize that our data are not precise enough to  
457 allow further discussion on Common Era sea level, therefore we maintain that future studies  
458 should be directed at finding more sea level indicators spanning this time frame, and  
459 measuring them with higher accuracy to allow for higher resolution sea level reconstructions.

460

461

#### 462 Author contributions

463 MB organized fieldwork and sampling that was conducted in collaboration with TM and DK. JJ gave on-  
464 site support in Makassar. MB led data analysis, with supervision from TM and AR. TS analyzed the tidal  
465 datum and MSL; PS offered expertise, models and discussion input on Glacial Isostatic Adjustment  
466 processes. MB wrote the manuscript with inputs from AR. All authors revised and approved the  
467 content.

468

#### 469 Declaration of Interest

470 The authors declare no conflict of interest

471

#### 472 7. Data availability

473 The data will be available in the data repository PANGEA and we will add the DOI when the MS gets  
474 to its final stage.

475



476 Acknowledgments

477 We would like to thank SEASCHANGE (RO-5245/1-1) from the Deutsche Forschungsgemeinschaft  
478 (DFG), which is part of the Special Priority Program (SPP)-1889 "Regional Sea Level Change and Society"  
479 for supporting this work. Thanks to Thomas Lorscheid and Deirdre Ryan for help and thoughtful  
480 comments. We acknowledge the help of the following Indonesian students and collaborators: Andi Eka  
481 Puji Pratiwi "Wiwi", Supardi and Veronica Lepong Purara, who provided support during fieldwork and  
482 sampling. We are grateful to the Indonesian Ministry for Research, Technology and Higher Education  
483 (RISTEKDIKTI) for assistance in obtaining research permits. The fieldwork for this study was conducted  
484 under Research Permit No. 311/SIP/FRP/E5/Dit.KI/IX/2017. We are also grateful to the Badan  
485 Informasi Geospasial (BIG), Indonesia, for sharing Makassar tide gauge data.

486

487

488

489 8. References

- 490 Azmy, K., Edinger, E., Lundberg, J. and Diegor, W.: Sea level and paleotemperature records from a  
491 mid-Holocene reef on the North coast of Java, Indonesia, *Int. J. Earth Sci.*, 99, 231–244,  
492 doi:10.1007/s00531-008-0383-3, 2010.
- 493 Baeda, A. Y.: Seismic and Tsunami Hazard Potential in Sulawesi Island , Indonesia, *J. Int. Dev. Coop.*,  
494 17(1), 17–30, 2011.
- 495 Bird, P.: An updated digital model of plate boundaries, *Geochemistry, Geophys. Geosystems*, 4(3),  
496 doi:10.1029/2001GC000252, 2003.
- 497 De Boer, B., Dolan, A. M., Bernales, J., Gasson, E., Goelzer, H., Golledge, N. R., Sutter, J. and  
498 Huybrechts, P.: Simulating the Antarctic ice sheet in the late-Pliocene warm period : PLISMIP-ANT ,  
499 an ice-sheet model intercomparison project , 881–903, doi:10.5194/tc-9-881-2015, 2015.
- 500 De Boer, B., Stocchi, P., Whitehouse, P. L. and Wal, R. S. W. Van De: Current state and future  
501 perspectives on coupled ice-sheet e sea-level modelling, *Quat. Sci. Rev.*, 169, 13–28,  
502 doi:10.1016/j.quascirev.2017.05.013, 2017.
- 503 Durrant, T., Hemer, M., Trenham, C., & Greenslade, D.: CAWCR Wave Hindcast 1979–2010. Data  
504 Collection, (2013).  
505
- 506 Durrant, T., Hemer, M., Smith, G., Trenham, C., Greenslade, D.: CAWCR Wave Hindcast extension  
507 June 2013 - July 2014. v1. CSIRO. Data Collection. <https://doi.org/10.4225/08/55C99193B3A63>,  
508 (2015)
- 509 Clark, J. A. and Farrell, W. E.: On Postglacial Sea Level, , 647–667, 1976.
- 510 Fieux, M., Andri, C., Charriaud, E., Ilahude, A. G., Metz, N., Molcard, R. and Swallow, J. C.:  
511 Hydrological and chloroflouromethane measurements of the Indonesian throughflow entering the  
512 Indian Ocean, , 101, 1996.
- 513 Godfrey, J. S.: The effect of the Indonesian throughflow on ocean circulation and heat exchange with  
514 the atmosphere- A review-Godfrey 1996.pdf, , 101, 1996.
- 515 Goodwin, I. D. and Harvey, N.: Subtropical sea-level history from coral microatolls in the Southern  
516 Cook Islands , since 300 AD, , 253, 14–25, doi:10.1016/j.margeo.2008.04.012, 2008.
- 517 Grossman, E. E., Fletcher, C. H. and Richmond, B. M.: The Holocene sea-level highstand in the



- 518 equatorial Pacific: Analysis of the insular paleosea-level database, *Coral Reefs*, 17(3), 309–327,  
519 doi:10.1007/s003380050132, 1998.
- 520 Hallmann, N., Camoin, G., Eisenhauer, A., Botella, A., Milne, G. A., Vella, C., Samankassou, E., Pothin,  
521 V., Dussouillez, P., Fleury, J. and Fietzke, J.: Ice volume and climate changes from a 6000 year sea-  
522 level record in French Polynesia, *Nat. Commun.*, 9(1), 1–12, doi:10.1038/s41467-017-02695-7, 2018.
- 523 Harris, R. O. N. and Major, J.: Waves of destruction in the East Indies : the Wichmann catalogue of  
524 earthquakes and tsunami in the Indonesian region from 1538 to 1877, , 9–46, 2017.
- 525 Houghton, J. T., Meiro Filho, L. G., Callander, B. A., Harris, N., Kattenburg, A., & Maskell, K. Climate  
526 change 1995: the science of climate change. *Climatic Change*, 584, (1996).  
527
- 528 IPCC: IPCC, 2014: Climate Change 2014: Synthesis Report. Contribution of Working Groups I, II and III  
529 to the Fifth Assessment Report of the Intergovernmental Panel on Climate Change [Core Writing  
530 Team, R.K. Pachauri and L.A. Meyer (eds.)]. IPCC, Geneva, Switzer, Ipcc, 31,  
531 doi:10.1017/CBO9781107415324, 2014.
- 532 Janßen, A., Wizemann, A., Klicpera, A. and Satari, D. Y.: Sediment Composition and Facies of Coral  
533 Reef Islands in the Spermonde Archipelago , Indonesia, , 4(May), 1–13,  
534 doi:10.3389/fmars.2017.00144, 2017.
- 535 Jones, E. S., Hayes, G. P., Bernardino, M., Dannemann, F. K., Furlong, K. P., Benz, H. M., Villaseñor, A.  
536 and Sea, M.: Seismicity of the Earth 1900 – 2012 Java and Vicinity : U.S. Geological Survey, , Open-  
537 File, 1, sheet, scale 1:5.000.000, doi:https://dx.doi.org/10.3133/ofr20101083N, 2014.
- 538 Kench, P. S. and Mann, T.: Reef Island Evolution and Dynamics: Insights from the Indian and Pacific  
539 Oceans and Perspectives for the Spermonde Archipelago, *Front. Mar. Sci.*, 4(May),  
540 doi:10.3389/fmars.2017.00145, 2017.
- 541 Khan, N. S., Ashe, E., Shaw, T. A., Vacchi, M., Walker, J., Peltier, W. R., Kopp, R. E. and Horton, B. P.:  
542 Holocene Relative Sea-Level Changes from Near-, Intermediate-, and Far-Field Locations, *Curr. Clim.*  
543 *Chang. Reports*, 1(4), 247–262, doi:10.1007/s40641-015-0029-z, 2015.
- 544 De Klerk, L. G.: Zeespiegel Riffen en Kustflakten in zuitwest Sulawesi, Indonesia, Utrecht., 1982.
- 545 Kopp, R. E., Horton, B. P., Kemp, A. C. and Tebaldi, C.: Past and future sea-level rise along the coast of  
546 North Carolina, USA, *Clim. Change*, 132(4), 693–707, doi:10.1007/s10584-015-1451-x, 2015.
- 547 Kopp, R. E., Kemp, A. C., Bittermann, K., Horton, B. P., Donnelly, J. P., Gehrels, W. R., Hay, C. C.,  
548 Mitrovica, J. X., Morrow, E. D. and Rahmstorf, S.: Temperature-driven global sea-level variability in  
549 the Common Era, *Proc. Natl. Acad. Sci.*, 113(11), E1434 LP-E1441, doi:10.1073/pnas.1517056113,  
550 2016.
- 551 Lambeck, K. and Chappell, J.: Sea level change through the last glacial cycle., , 292(5517), 679–686,  
552 doi:10.1126/science.1059549, 2001.
- 553 Mann, T., Rovere, A., Schöne, T., Klicpera, A., Stocchi, P., Lukman, M. and Westphal, H.: The  
554 magnitude of a mid-Holocene sea-level highstand in the Strait of Makassar, *Geomorphology*, 257,  
555 155–163, doi:10.1016/j.geomorph.2015.12.023, 2016.
- 556 Mcgregor, H. V, Fischer, M. J., Gagan, M. K., Fink, D. and Woodroffe, C. D.: Environmental control of  
557 the oxygen isotope composition of Porites coral microatolls, *Geochim. Cosmochim. Acta*, 75(14),  
558 3930–3944, doi:10.1016/j.gca.2011.04.017, 2011.
- 559 Meltzner, A. J. and Woodroffe, C. D.: Coral microatolls, in *Handbook of Sea-level Research*, Wiley  
560 Chichester., 2014.



- 561 Meltzner, A. J., Switzer, A. D., Horton, B. P., Ashe, E., Qiu, Q., Hill, D. F., Bradley, S. L., Kopp, R. E., Hill,  
562 E. M., Majewski, J. M., Natawidjaja, D. H. and Suwargadi, B. W.: Half-metre sea-level fluctuations on  
563 centennial timescales from mid-Holocene corals of Southeast Asia, *Nat. Commun.*, 8, 14387,  
564 doi:10.1038/ncomms14387, 2017.
- 565 Milne, G. A. and Mitrovica, J. X.: Searching for eustasy in deglacial sea-level histories, *Quat. Sci. Rev.*,  
566 27(25–26), 2292–2302, doi:10.1016/j.quascirev.2008.08.018, 2008.
- 567 Milne, G. A., Gehrels, W. R., Hughes, C. W. and Tamisiea, M. E.: Identifying the causes of sea-level  
568 change, *Nat. Geosci.*, 2(7), 471–478, doi:10.1038/ngeo544, 2009.
- 569 Mitrovica, J. X. and Milne, G. A.: On the origin of late Holocene sea-level highstands within equatorial  
570 ocean basins, *Quat. Sci. Rev.*, 21(20–22), 2179–2190, doi:10.1016/S0277-3791(02)00080-X, 2002.
- 571 Mitrovica, J. X. and Peltier, W. R.: On Postglacial Geoid Subsidence Over the Equatorial Oceans, ,  
572 96(91), 53–71, 1991.
- 573 Nicholls, R. J. and Cazenave, A.: Sea-level rise and its impact on coastal zones, *Science* (80-. ),  
574 328(5985), 1517–1520, doi:10.1126/science.1185782, 2010.
- 575 Nicholls, R. J., Hoozemans, F. M. J. and Marchand, M.: Increasing flood risk and wetland losses due to  
576 global sea-level rise: Regional and global analyses, *Glob. Environ. Chang.*, 9(SUPPL.),  
577 doi:10.1016/S0959-3780(99)00019-9, 1999.
- 578 Peltier, W. R.: GLOBAL GLACIAL ISOSTASY AND THE SURFACE OF THE ICE-AGE EARTH: The ICE-5G  
579 (VM2) Model and GRACE, *Annu. Rev. Earth Planet. Sci.*, 32(1), 111–149,  
580 doi:10.1146/annurev.earth.32.082503.144359, 2004.
- 581 Peltier, W. R.: Closure of the budget of global sea level rise over the GRACE era: the importance and  
582 magnitudes of the required corrections for global glacial isostatic adjustment, *Quat. Sci. Rev.*, 28(17–  
583 18), 1658–1674, doi:10.1016/j.quascirev.2009.04.004, 2009.
- 584 Prasetya, G. S., De Lange, W. P. and Healy, T. R.: The Makassar Strait Tsunamigenic region, Indonesia,  
585 *Nat. Hazards*, 24(3), 295–307, doi:10.1023/A:1012297413280, 2001.
- 586 Reimer, P. J., Bard, E., Bayliss, A., Beck, J. W., Blackwell, P. G., Bronk Ramsey, C., Buck, C. E., Cheng,  
587 H., Edwards, R. L., Friedrich, M., Grootes, P. M., Guilderson, T. P., Hafliadason, H., Hajdas, I., Hatté, C.,  
588 Heaton, T. J., Hoffmann, D. L., Hogg, A. G., Hughen, K. A., Kaiser, K. F., Kromer, B., Manning, S. W.,  
589 Niu, M., Reimer, R. W., Richards, D. A., Scott, E. M., Southon, J. R., Staff, R. A., Turney, C. S. M. and  
590 van der Plicht, J.: IntCal13 and Marine13 Radiocarbon Age Calibration Curves 0–50,000 Years cal BP,  
591 *Radiocarbon*, 55(4), 1869–1887, doi:10.2458/azu\_js\_rc.55.16947, 2013.
- 592 Rhodes, B. P., Kirby, M. E., Jankaew, K. and Choowong, M.: Evidence for a mid-Holocene tsunami  
593 deposit along the Andaman coast of Thailand preserved in a mangrove environment, *Mar. Geol.*,  
594 282(3–4), 255–267, doi:10.1016/j.margeo.2011.03.003, 2011.
- 595 Sawall, Y., Teichberg, M. C., Seemann, J., Litaay, M., Jompa, J. and Richter, C.: Nutritional status and  
596 metabolism of the coral *Stylophora subseriata* along a eutrophication gradient in Spermonde  
597 Archipelago (Indonesia), *Coral Reefs*, 30(3), 841–853, doi:10.1007/s00338-011-0764-0, 2011.
- 598 Schwerdtner Máñez, K., Husain, S., Ferse, S. C. A. and Máñez Costa, M.: Water scarcity in the  
599 Spermonde Archipelago, Sulawesi, Indonesia: Past, present and future, *Environ. Sci. Policy*, 23, 74–  
600 84, doi:10.1016/j.envsci.2012.07.004, 2012.
- 601 Schöne, T., Esselborn, S., Rudenko, S., Raimondo, J.-C.: Radar Altimetry derived Sea Level Anomalies -  
602 the Benefit of new Orbits and Harmonization, in: Flechtner et al. (eds.) *System Earth via Geodetic-*  
603 *Geophysical Space Techniques*, Series: Advanced Technologies in Earth Sciences, doi: 10.1007/978-3-  
604 642-10228-8 25 (2010)



- 605 Scoffin, T. P. and Stoddart, D. R.: The nature and significance of microatolls, *Philos. Trans. R. Soc.*  
606 *London, Ser. B, Biol. Sci.*, 284(999), 99–122, 1978.
- 607 Shennan, I. A. N.: Flandrian sea-level changes in the Fenland . II : Tendancies of sea-level movement ,  
608 altitudinal changes , and local and regional factors , , 1(200), 1986.
- 609 Smithers, S. G. and Woodroffe, C. D.: Coral microatolls and 20th century sea level in the eastern  
610 Indian Ocean, *Earth Planet. Sci. Lett.*, 191(1–2), 173–184, doi:10.1016/S0012-821X(01)00417-4, 2001.
- 611 Southon, J., Kashgarian, M., Fontugne, M., Metivier, B. and Yim, W. W. S.: Marine reservoir  
612 corrections for the Indian Ocean and Southeast Asia, *Radiocarbon*, 44(1), 167–180,  
613 doi:10.1017/S0033822200064778, 2002.
- 614 Spada, G. Ā. and Stocchi, P.: SELEN : A Fortran 90 program for solving the ““ sea-level equation ”” \$ , ,  
615 33, 538–562, doi:10.1016/j.cageo.2006.08.006, 2007.
- 616 Syamsir, Birawida, A. B. and Faisal, A.: Development of Water Quality Index of Island Wells in  
617 Makassar City, *J. Phys.*, (1155), doi:10.1088/1742-6596/1155/1/012106, 2019.
- 618 Thein, P. S., Pramumijoyo, S., Wilopo, W., Setianto, A. and Sri, K.: ESTIMATION OF SUBSURFACE  
619 STRUCTURE BASED ON MICROTREMOR , BORE HOLE OBSERVATIONS AND STOCHASTIC STRONG  
620 GROUND MOTION SIMULATIONS IN PALU CITY , CENTRAL SULAWESI , INDONESIA : A VALIDATION  
621 AND SENSITIVITY STUDY ON THE 23 JANUARY 2005 ( PALU ) EARTHQUAKE , , 6(2), 96–108, 2014.
- 622 Tjia, H. D., Fujii, S., Kigoshi, K., Sugimura, A. and Zakaria, T.: Radiocarbon dates of elevated shorelines,  
623 Indonesia and Malaysia. Part 1, *Quat. Res.*, 2(4), 487–495, doi:10.1016/0033-5894(72)90087-7, 1972.
- 624 Vitousek, S., Barnard, P. L., Fletcher, C. H., Frazer, N., Erikson, L. and Storlazzi, C. D.: Doubling of  
625 coastal flooding frequency within decades due to sea-level rise, *Sci. Rep.*, 7(1), 1–9,  
626 doi:10.1038/s41598-017-01362-7, 2017.
- 627 Walpersdorf, A., Vigny, C., Manurung, P., Subarya, C. and Sutisna, S.: Determining the Sula block  
628 kinematics in the triple junction area in Indonesia by GPS, 1998.
- 629 Wessel, P. and Smith, W. H. F.: A global, self-consistent, hierarchical, high-resolution shoreline  
630 database, *J. Geophys. Res. Solid Earth*, 101(B4), 8741–8743, doi:10.1029/96jb00104, 2004.
- 631 Woodroffe, C. D.: Mid-late Holocene El Niño variability in the equatorial Pacific from coral  
632 microatolls, *Geophys. Res. Lett.*, 30(7), 1–4, doi:10.1029/2002GL015868, 2003.
- 633 Woodroffe, C. D., McGregor, H. V., Lambeck, K., Smithers, S. G. and Fink, D.: Mid-Pacific microatolls  
634 record sea-level stability over the past 5000 yr, *Geology*, 40(10), 951–954, doi:10.1130/G33344.1,  
635 2012.
- 636 Woodroffe, S. A., Long, A. J., Lecavalier, B. S., Milne, G. A. and Bryant, C. L.: Using relative sea-level  
637 data to constrain the deglacial and Holocene history of southern Greenland, *Quat. Sci. Rev.*, 92, 345–  
638 356, doi:10.1016/j.quascirev.2013.09.008, 2014.
- 639 Woodroffe, S. A., Long, A. J., Milne, G. A., Bryant, C. L. and Thomas, A. L.: New constraints on late  
640 Holocene eustatic sea-level changes from Mahé, Seychelles, *Quat. Sci. Rev.*, 115, 1–16,  
641 doi:10.1016/j.quascirev.2015.02.011, 2015.
- 642 Zachariasen, J.: Paleoseismology and Paleogeodesy of the Sumatra Subduction Zone: A Study of  
643 Vertical Deformation Using Coral Micoatolls, 1998.
- 644